Original Research

Magnetic resonance imaging tracking of ultra small superparamagnetic iron oxide labeled rabbit dendritic cells

Jing Zhou[1], Fuyuan Yang[1], Quan Zhou[2], Kanrong Yang[2] and Wenli Chen[1]

[1]College of Biophotonics, South China Normal University, Guangzhou 510631, China; [2]Medical Imaging Center, First Affiliated Hospital of Jinan University, Guangzhou 510631, China

Corresponding author: Wenli Chen. Email: chenwl@scnu.edu.cn

Abstract

Dendritic cells (DCs) play an important role in atherosclerosis plaque formation, but the mechanism has not been elucidated clearly. This study is designed to establish a method for tracing DCs *in vivo* facilitating the investigation of the DCs' specific roles in atherosclerosis. Rabbit DCs labeled by different concentrations of ultra small superparamagnetic iron oxide (USPIO) were injected into atherosclerosis rabbit model and traced with magnetic resonance imaging (MRI). Results showed that USPIO labeling nearly have no cytotoxicity to DCs in low concentrations ($<$500 μg/mL) but induced some decrease of cell viability at high concentrations ($>$500 μg/mL). Moreover, USPIO labeling, from 200 to 2000 μg/mL, caused a dose-dependent decrease of the mitochondrial membrane potential in DCs. The high labeling concentration (2000 μg/mL) triggered necrosis instead of apoptosis in DCs. By T2WI and fs T2WI sequence imaging comparison, DCs were found to exist in rabbit abdominal artery plaques after 24 h of transplantation and in spleen after one week detected by Prussian blue staining of tissue sections. We concluded that about 200 μg/mL USPIO is ideal to effectively label DCs for MRI tracing *in vivo* without a threat to cell viability. Combining USPIO labeling and MRI to track the movement of injected DCs *in vivo* is a feasible method.

Keywords: Ultra small superparamagnetic iron oxide, dendritic cells, atherosclerotic rabbit model, magnetic resonance imaging

***Experimental Biology and Medicine* 2014; 239: 13–23. DOI: 10.1177/1535370213508712**

Introduction

Immune response plays an important role in atherosclerosis plaque formation which involves many infiltration materials, such as leukocytes, macrophagocytes, and T lymphocytes.[1–3] Dendritic cells (DCs), as the most powerful antigen-presenting cells, also participate in atherosclerosis plaque formation.[4] DCs exist throughout the body including the thymus, blood, lymph, and most visceral organs to work as immune sentinels responding to invading pathogens in tissues.[5,6] In the formation of atherosclerosis, immature DCs (iDCs) were recruited to atherosclerotic lesion and then induced into maturation state by ox-LDL, advanced glycation end products, and C-reactive protein (CRP) in atherosclerosis plaque.[7–9] Then, the mature DCs were engaged in presenting antigens to T lymphcytes and starting the cascade reactions or inducing production of proteases such as metalloproteinases which disintegrate the extracellular matrix.[10,11] It has been reported that atherosclerosis plaque buildup could be suppressed by decreasing the assembling of DCs.[12] However, the molecular mechanism of DCs accelerating the formation of atherosclerosis still needs to be further elucidated. And what more interesting is that immature DCs may participate in suppressing rather than accelerating immune responses in atherosclerosis formation in a way that they are employed nowadays for cancer immunotherapy.[13] Therefore, developing experimental approaches to trace the migration of transplanted DCs in atherosclerotic animal models may facilitate the investigation of the DCs' specific roles in atherosclerosis as well as their promising usage for atherosclerosis immunotherapy.

Cooperating with contrast agent labeling, magnetic resonance imaging (MRI) has been successfully used to track transplanted cells *in vivo* for its high spatial resolution.[14,15] Iron oxide nanoparticles are able to cause signal decrease on mid T1-/T2- and T2*-weighted MRI and widely used as a sort of contrast agents in cell tracing.[15] Ultra-superparamagnetic iron oxide (USPIO) is a kind of iron oxide nanoparticle with a diameter of 30–50 nm. UAPIO was thought to have a relatively long half life than larger superparamagnetic iron oxide (SPIO) particles, such as SPIO and micron-sized iron oxide particles (MPIO), which make it an effective contrast agent in vascular imaging.[16–18] Considering common drawbacks of direct cell labeling, such as cytotoxicity, proliferation and differentiation capacity damage,[18] the labeled DCs' viability and function need to be understood.

Copyright © 2013 by the Society for Experimental Biology and Medicine

Here, we studied the feasibility of tracking USPIO-labeled DCs in atherosclerosis rabbit model. Our results showed that USPIO labeling would cause a significant loss of cell activity via necrosis at high concentrations but not at low concentrations which could also effectively label DCs to cause negative signal in MRI scanning *in vitro* and *in vivo*. Importantly, in atherosclerosis rabbits, transplanted USPIO-labeled DCs were tracked in inflammatory plaque at 24 h and in spleen in one week.

Materials and Methods

Animals

New Zealand white rabbits (aged 3 months, 2–2.5 kg) were obtained from the Laboratory Animal Center of Guangdong province. The rabbits were randomly divided into three groups: control group ($n = 6$), fed with a regular normal diet (120 g per rabbit per day) for 12 weeks; atherosclerosis blank group ($n = 6$), fed with a regular high fat diet (120 g per rabbit per day) supplemented with 5% (w/w) cholesterol and 10% (w/w) lard for 12 weeks; and DCs transplant group ($n = 6$), the atherosclerosis rabbits transplanted with USPIO-labeled DCs. BSA (2.5 mg/kg) was injected into rabbits in the atherosclerosis rabbits via ear vein every four weeks. Animal procedures were performed in accordance with the guidelines set by the Animal Experiment Committee of Southern China Normal University Guangzhou, China.

Preparation and identification of DCs

Peripheral blood mononuclear cells (PBMC) were isolated from rabbit peripheral blood by density-gradient centrifugation using Ficoll-Hypaque centrifugation. Monocytes were isolated by their adherence to plastic from PBMC and then induced for differentiation into DCs in RPMI 1640 (Life Technologies Inc., Grand Island, NY) supplemented with 100 U/mL penicillin/streptomycin, 10% FBS, 50 ng/mL granulocyte-macrophage colony-stimulating factor (GM-CSF), and 50 ng/mL interleukin-4 (IL-4) (PeproTech, Rocky Hill, NJ). After cultured for nine days, with the medium refreshed every three days, cells were morphologically identified with an optical microscope and molecularly identified with flow cytometry after being labeled with anti-CD86-FITC and anti-HLA-DR-PE.

USPIO labeling

USPIO, with a size of 30–50 nm, was provided by Prof. Xu Yikai (Department of Medical Imaging Center, Nan Fang Hospital, Southern Medical University). It was prepared by stabilizing iron oxide (Fe_2O_3) particles with carboxydextran and sodium citrate, and supplied at a concentration of 20 mg Fe/mL. USPIO was incubated with 1.5 μg/mL poly-L-lysine (PLL) (Sigma, St Louis, MO, USA) in RPMI 1640 medium without FBS for 30 min before usage. DCs (5×10^5 cells/well) were incubated with different concentrations of USPIO-DLL in RPMI 1640 medium without FBS for 24 h. Then the cells were subjected to experiments. The labeling efficiency, i.e. iron content within the USPIO-labeled DCs was quantified by atomic absorption spectrometry (AAS) using a polarized Zeeman atomic absorption spectrometer (Hitachi, Model Z-8200, Japan).

Cytotoxicity and cell death type assay

Cell Counting Kit-8 (CCK-8, Dojindo Laboratories, Kumamoto, Japan) assay was used to evaluate DCs' viability. All experiments were performed in quintuplicate on three separate occasions. The survival rate was expressed as a percentage (mean OD_{450} of treated cells/mean OD_{450} of control cells).

Annexin V-FITC/PI Kit (BD Co., San Jose, USA) was used to detect cell apoptosis and necrosis. Experiment was conducted following manufacturer's instructions. Samples were detected with a flow cytometer (FACS CantoTM, BD Co. Inc., Franklin Lakes, NJ). The cells with Annexin V-FITC−/PI− were classified as health cells, Annexin V-FITC+/PI− as apoptotic cells, Annexin V-FITC+/PI+ as late apoptotic or necrotic cells, and Annexin V-FITC−/PI+ as necrotic cells.

Detection of mitochondrial membrane potential

Mitochondrial membrane potential (MMP) was detected by Rhodamine 123 staining (Alexis Biochemicals Inc, San Diego, CA). Control cells and USPIO-labeled cells were collected and incubated with 5 μM Rhodamine 123 for 30 min in the dark and then washed three times with PBS. MMP changes were determined from Rhodamine 123 fluorescence which was detected by flow cytometry.

In vitro MRI of USPIO-labeled DCs

SPIO-labeled cells were transferred into 1.5 mL Eppendorf tubes loaded with 1 mL of 1% agarose. Unlabeled cells of the same densities were processed as the same manner to serve as the negative control. MR imaging was performed on a 1.5T MRI (GE Sigma HD 1.5T MR) with a 12.7 cm receive-only knee coil. DCs (1×10^6) labeled with 200 μg/mL USPIO were imaged using a fast spin echo T2 sequence (repetition time ms/echo time [ms] = 4000/108, 16 echo train length) and a spin echo T1 sequence (repetition time ms/echo time [ms] = 500/17.9) with the section thickness of 2 mm and field of view (FOV) of $13 \times 13\ cm^2$. Images were obtained with a matrix size of 256×256. Region of interest (ROI) for signal intensity (SI) measurement was $14.6\ mm^2$. The percentage change of SI (ΔSI) was calculated by using the equation:

$$\Delta SI = (SI_l - SI_{ul})/SI_{ul} \times 100\%$$

where SI_l and SI_{ul} are the SI of the labeled cells and unlabeled cells, respectively.

In vivo MRI tracking of DCs

All the rabbits were performed MRI for atherosclerosis identification. Subsequently, 200 μg/mL USPIO labeled DCs were injected into the DCs transplant group rabbits via ear vein (5×10^6 cells/mL, 2 mL per rabbit), while same amount of physiological saline was injected into rabbits in the control group and blank group. MRI tracing was

performed in T2WI and fs T2WI sequence 24 h after injection. Increases in signal intensity (SI) enhancement were measured in defined regions of interest (ROI) for SI measurement. MR imaging was performed with knee coil on a 1.5T MRI with 3/0.5 mm slice thickness. MRI scanning parameters: (1) T_2WI sequence: TR = 2500 ms, TE = 2500 ms, FOV = 14.0 mm, with a matrix size of 256 × 256; (2) fs T_2WI sequence: TR = 2500 ms, TE = 2500 ms, FOV = 14.0 mm, with a matrix size of 256 × 256.

Pathological and histological examination

One week after MRI tracking, abdominal aorta and spleen tissue from control group, atherosclerosis blank group, and DCs transplant group were fixed, paraffin-embedded, and sliced for histological examination. HE and Prussian blue staining were performed respectively. Intima of atherosclerotic rabbit, iron accumulation in blood vessel wall, and inner plaque were observed.

Serum lipid analysis

After fed for 12 weeks, rabbits from control group, atherosclerosis blank group, and DCs transplant group (before DCs injection) were subjected to blood biochemical analysis. An automated biochemical analyzer (Type AU5421, Olympus, Japan) was used for estimation of the concentrations of triglycerides (TG), total cholesterol (TC), low density lipoprotein cholesterol (LDL-C), and high density lipoprotein cholesterol (HDL-C) in plasma.

Statistical analysis

Each experiment was repeated at least three times. Data were presented as mean ± SD. Statistical analyses were carried out by SPSS 12 (SPSS, Chicago) using one way ANOVA analysis (Bonferroni correction). $P < 0.05$ was considered as statistical significance.

Results

Establishment of atherosclerotic rabbit models

The atherosclerosis rabbits were fed with a regular high fat diet (120 g per rabbit per day) supplemented with 5% (w/w) cholesterol and 10% (w/w) lard for 12 weeks. Then the blood lipids content were detected and atherosclerosis rabbits have marked increase of blood lipids content compared with control group (Table 1). Except TG content, TC, HDL-C, and LDL-C contents were largely increased in atherosclerosis rabbits compared to control rabbits. The formation of atherosclerosis was also confirmed by artery cross-section histological analysis. As shown in Figure 1, intima of rabbits in the control group was relatively smooth in contrast to thick and upheaved in the atherosclerosis group. Furthermore, the cells under intima of control rabbits showed a normal shape, a close connection, and a good order, but which featured unorganized arrangement and higher dispersion in atherosclerosis rabbits (Figure 2). Figure 2 also showed the inflammatory cell infiltration below the arterial endothelial cell layer. All of those suggested a classic severe neointimal hyperplasia.

Identification of DCs

PBMC were isolated from rabbit peripheral blood by density-gradient centrifugation, and monocytes were isolated by their adherence to plastic from PBMC and then induced for differentiation into DCs in RPMI 1640 supplemented with growth factors for nine days. DCs identification was determined from the morphology of cultured cells and examination of cell surface molecules. On the third day of inducing differentiation culture, cells showed a decreased adherence to plastic, clumped together. On the sixth day of culture, the cells became larger and exhibited irregular shape. On the ninth day, cells exhibited more typical dendritic morphology and most cells were suspended with a rough cell surface with a lot of wrinkles (Figure 3). They were morphologically typical of DCs. Besides, expressions of CD86 and HLA-DR on cell surface were detected at 3 and 9 days of culture. As shown in Figure 4, from the third to the ninth day, the expressions of CD86 and HLA on cell surface were significantly upregulated. All these data defined typical DCs.

Effect of USPIO labeling on DCs

CCK8 assay was performed to evaluate the effect of USPIO labeling on DCs' viability. As shown in Figure 5, exposure to 0–200 μg/mL USPIO for 24 h hardly affected DCs' viability and 500 μg/mL USPIO modestly impaired cell viability but was not statistically significant. However, higher concentrations of USPIO (>500 μg/mL) induced significant loss of cell viability. Consistent with the CCK8 results, Annexin V-FITC/PI assay showed that only 2000 μg/mL USPIO incubation for 24 h induced a higher ratio of DCs necrosis (18.5% more than control) but not apoptosis (2.6% more than control). The lower concentrations of USPIO (0–500 μg/mL) showed no cytotoxicity to DCs (Figure 6).

Table 1 Serum lipid analysis of the rabbit models

Groups	TC	TG	HDL-C	LDL-C
Control group	1.11 ± 0.50	0.85 ± 1.02	0.47 ± 0.18	0.59 ± 0.31
Atherosclerosis blank group	33.06 ± 1.07	0.80 ± 0.59	2.51 ± 0.54	23.39 ± 5.68
DCs transplant group (before transplant)	33.33 ± 0.73	0.63 ± 0.50	2.26 ± 0.70	23.00 ± 2.41

Note: Data are expressed as mean ± SD.
TC: total cholesterol; TG: triglycerides; HDL-C: high density lipoprotein cholesterol; LDL-C: low density lipoprotein cholesterol.

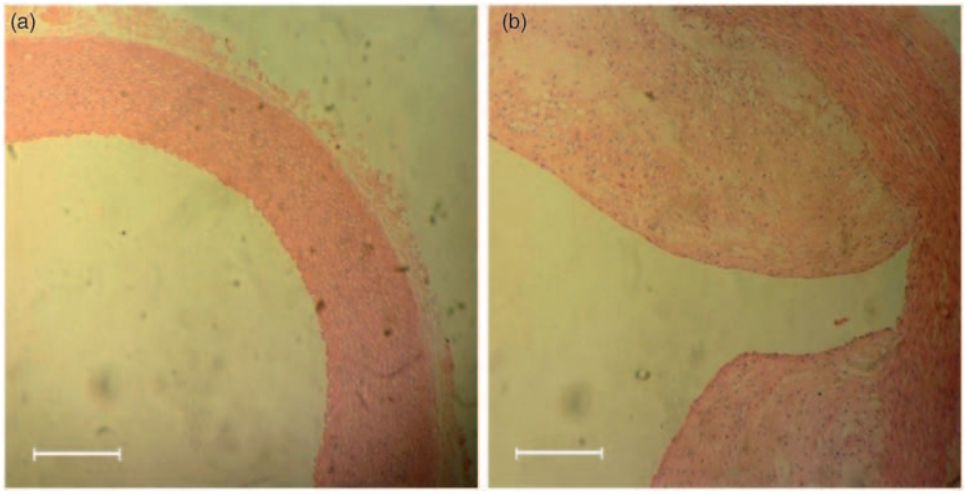

Figure 1 Abdominal artery sections of the rabbits in (a) the control group (b) and the atherosclerosis group under an optical microscope. The intima of rabbits in control group was smoother and thinner compared to those in atherosclerosis group with a protruding surface, suggesting a intimal hyperplasia in atherosclerosis group. Bars, 100 μm. (A color version of this figure is available in the online journal)

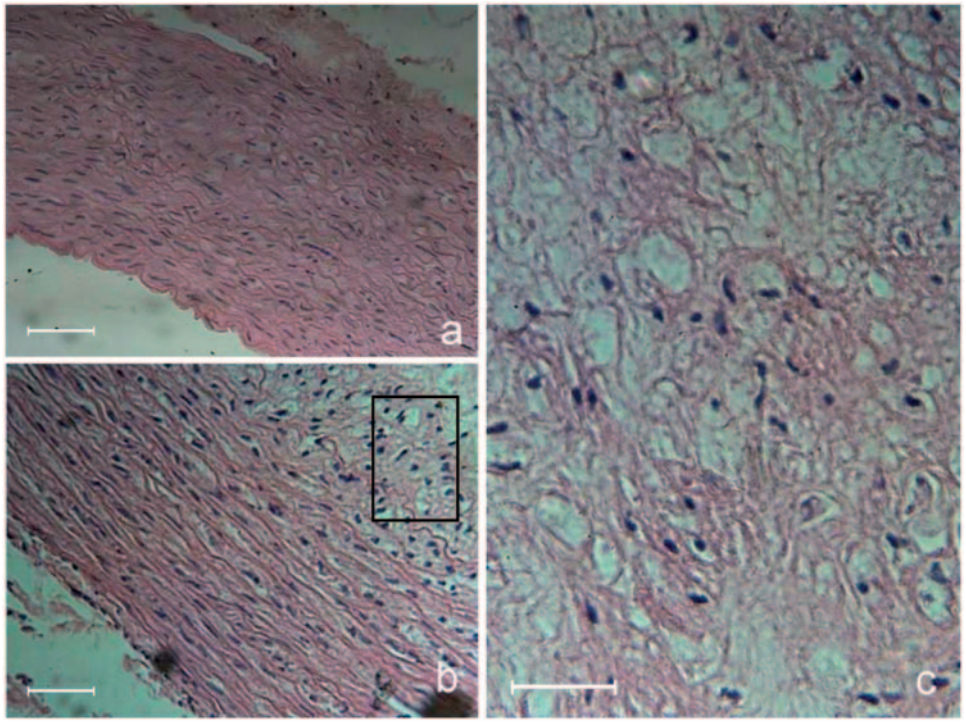

Figure 2 Photomicrographs of artery sections. Histological examination of vessel cross sections were obtained from the rabbit model in control rabbits (a) and atherosclerosis rabbits (b). For control rabbits section, cells under intima were neatly arranged, characterized by close connection and narrow spacing. For atherosclerosis rabbits section, the space between the cells significantly expanded and the cells arranged in a mess (c). Bars, 25 μm. (A color version of this figure is available in the online journal)

To explore whether the mitochondrial pathway involved in USPIO-labeling induced cell death, MMP was detected by Rhodamine 123 staining. Results showed that USPIO incubation (200, 500, 2000 μg/mL) induced significant decreases of MMP (7.5%, 15.6%, 21.8% more than control), indicating that a dose-dependent depolarization of MMP may be involved in USPIO-labeling-induced DCs necrosis (Figure 7).

Efficiency of USPIO labeling DCs

To evaluate the efficiency of USPIO labeling DCs, quantitative analysis of intracellular iron content was performed by atomic absorption spectroscopy (AAS). As showed in Figure 8, DCs intracellular iron content significantly increased with the USPIO incubation concentrations from 0 to 500 μg/mL. However, 1000 μg/mL USPIO labeling induced a decreased DCs intracellular iron content than

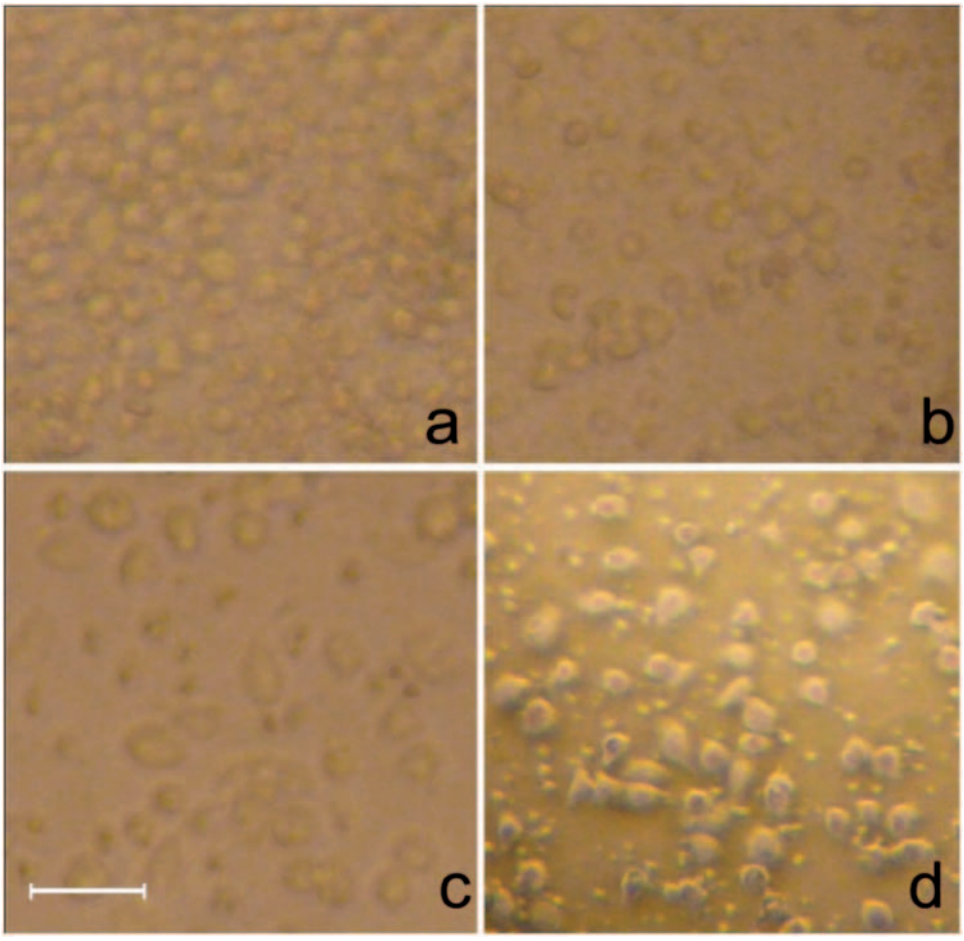

Figure 3 Morphology of cultured dendritic cells. Optical microscope photographs were obtained when the cells were just isolated (a), cultured for three days (b), six days (c), and nine days (d). After being cultured for three days, the cells aggregated, and most of the cells were suspended. In following six days, the cells became bigger and irregular, and burr-like projections began to appear in the cell surface. Bars, 50 μm. (A color version of this figure is available in the online journal)

100 μg/mL USPIO. Low concentrations USPIO could effectively label DCs while high dose USPIO showed relatively low intracellular iron content for cytotoxicity (Figures 5 and 6).

To evaluate the effect of USPIO labeling on MR imaging, after being labeled with 200 μg/mL USPIO for 24 h, DCs were imaged on a 1.5T MR-scanner using T1WI and T2WI sequence. Compared with unlabeled DCs, USPIO-labeled DCs showed significantly lower signal intensity in T2WI sequence but not T1WI (Figure 9(a) and (b)), which suggest that 200 μg/mL USPIO labeled DCs were sufficient to cause distinguishable signal change at 1.5T MRI at the density of 1×10^6/mL. Moreover, in this case, T2WI proved to be a sequence more responsive to signal change than T1WI.

MRI tracking of transplanted DCs in atherosclerotic rabbits

In order to determine the transplanted USPIO-DCs' location in atherosclerotic plaques, *in vivo* MRI scanning was performed. In this experiment, fs T2WI, which was the most sensitive sequence for identifying plaque, and T2WI, which has been proved to be a sequence more responsive to signal change than T1WI, were selected for scanning. In Figure 10, the plaques, the white area of the artery (red rectangle), were indicated by white arrow. The plaques of atherosclerosis blank rabbits and DCs transplant rabbits could be seen clearly in fs T2WI sequence. However, the plaques of DCs transplant rabbits were darker than that of atherosclerosis blank rabbits. Similarly, the plaques of atherosclerosis blank rabbits could be seen but blurrily in T2WI sequence while the plaques of DCs transplant rabbits could not be seen. These results suggested that the transplanted DCs migrated to the atherosclerosis plaque where the signal intensity was reduced.

To further study the migration state of DCs *in vivo*, spleen and vascular tissue of the transplanted rabbit were sliced one week after MRI for histological experiments and Prussian blue staining. Iron particles were not found in the vessel wall tissue, whereas they appeared in spleen (Figure 11), indicating a migration of DCs from plaque to spleen.

Discussion

DCs play an important role in the atherosclerosis plaque formation. Transplanting DCs into atherosclerosis models

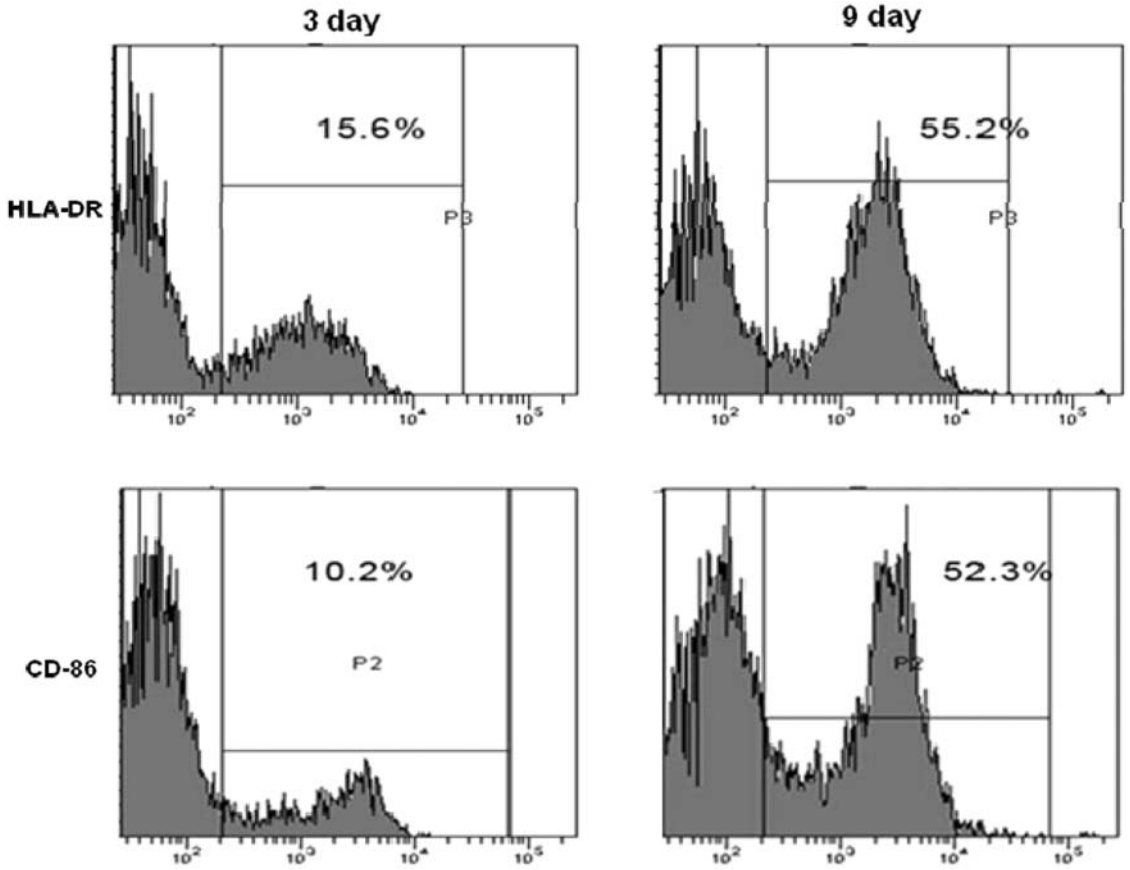

Figure 4 Detection of surface markers of DCs by flow cytometry. The expression of HLA-DR and CD86 on DCs cell membrane were detected by antibodies through flow cytometry analysis. DCs cultured for three and nine days were collected. Each figure is a representative of at least three experiments

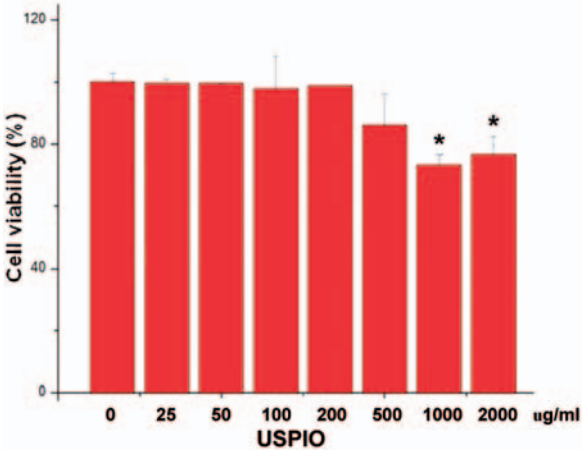

Figure 5 Effect of USPIO labeling on cell viability. Twenty-four hours after the DCs were labeled with the indicated concentrations of USPIO, cell viabilities were analyzed by CCK8. Cell viability of the control group which was cultured without SPIO was set as 100%. The graph is the representative of three experiments. *$P < 0.05$, compared to control. (A color version of this figure is available in the online journal)

and tracing their migration in the body is a promising method to investigate the specific role of DC in atherosclerosis *in vivo*. Moreover, studying the location and function of DCs labeled with different methodologies will promote their promising usage for atherosclerosis immunotherapy. In this study, we firstly investigated the feasibility of the method of MRI tracking of transplanted USPIO-labeled DCs in atherosclerosis rabbits. We concluded that about 200 μg/mL USPIO is ideal to effectively label DCs for MRI tracing *in vivo* without a threat to cell viability.

MRI is a non-invasive technique that can provide an ideal platform for tracking transplanted cells.[19] However, the transplanted cells must be labeled with a MR contrast for imaging. By surrounding with the polymer or polysaccharide shell, SPIO has been popularly used as a kind of negative contrast agent in MRI. Ultrasmall SPIO, with a diameter of 30–50 nm, are usually used for molecular imaging due to its relatively longer plasma-circulation time.[20] Moreover, Laland et al. have effectively tracked USPIO-labeled stem cells in vivo by MRI imaging.[21] In addition, anionic USPIO have a repulsive interaction with the cell surface because of the negative charge of the proteins on cell membrane. Previous studies have shown that PLL, a transfection agent, wrapped iron oxide particles through electrostatic interaction which functioned well in labeling cells.[22,23] In order to facilitate the cellular uptake of USPIO, we applied 1.5 μg/mL PLL to treat USPIO for 30 min at 37°C before usage.

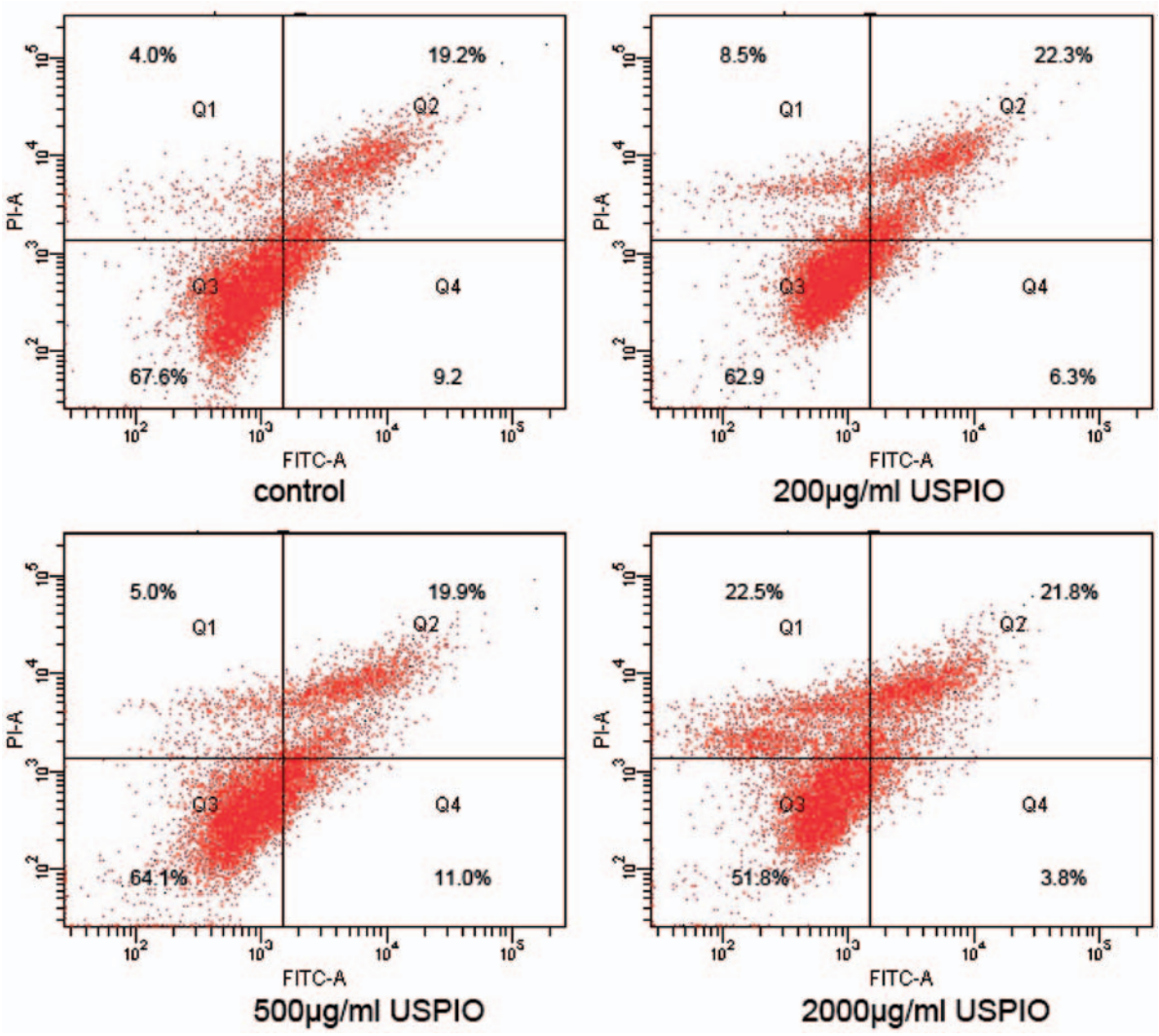

Figure 6 Type of DCs death induced by USPIO labeling. DCs were incubated with different concentrations of USPIO for 24 h. The type of cell death was detected by Annexin V-FITC/PI staining through flow cytometry. The cells with Annexin V-FITC−/PI− were health cells, Annexin V-FITC+/PI− were apoptotic cells, Annexin V-FITC+/PI+ were late apoptotic or necrotic cells, and Annexin V-FITC−/PI+ were necrotic cells. Results are representatives of three independent experiments. (A color version of this figure is available in the online journal)

The efficiency of USPIO labeling DCs assay showed that, in low concentration range, the amount of iron engulfed by DCs increased with the USPIO incubation concentrations. However, higher concentrations of USPIO incubation showed a decreased iron uptake. This may suggest that high concentrations of USPIO incubation reduce cell activity, which lead to a decreased iron uptake. For MRI threshold detection, DCs labeled with 200 μg/mL USPIO were collected for MRI scanning. The results showed that the cells could cause a distinguished signal decrease in MRI T2WI sequence but not in T1WI, for T1WI sequence needs more cell number or higher incubation concentration.

For the threshold of MRI detection of labeled DCs dependent on the amount of Fe/cell, a relatively high concentration of USPIO is required to label DCs for injection. Considering that cell viability was affected by high concentrations of USPIO, 200 μg/mL USPIO was chosen to label DCs for injection to perform MRI tracking *in vivo*. On the basis of previous experiments of cell transplantation and *in vivo* imaging, 2 mL of USPIO-labeled DCs (10^7 cells) was injected into a rabbit model via ear vein.[24,25]

MR imaging is an efficient clinical method for evaluation of soft tissues and a good way for measuring the level of inflammation and thrombosis.[26,27] T2WI fs sequence showed a high quality in plaque imaging as it shows a marked preference for fat. In our study, plaques of atherosclerosis rabbit get decreased signal in fs T2WI and T2WI imaging after the rabbit was transplanted into labeled DCs, which indicated that the transplanted DCs migrated to the atherosclerosis plaque. Prussian blue staining showed the presence of transplanted DCs in spleen after one week, suggesting a migration from inflamed tissues to secondary lymphatic organs, which is consistent with the general migration pattern of DCs.

It was reported that high concentrations of SPIO could induce cell apoptosis.[28,29] In this study, we demonstrated that USPIO did not cause cell death within a wide range of

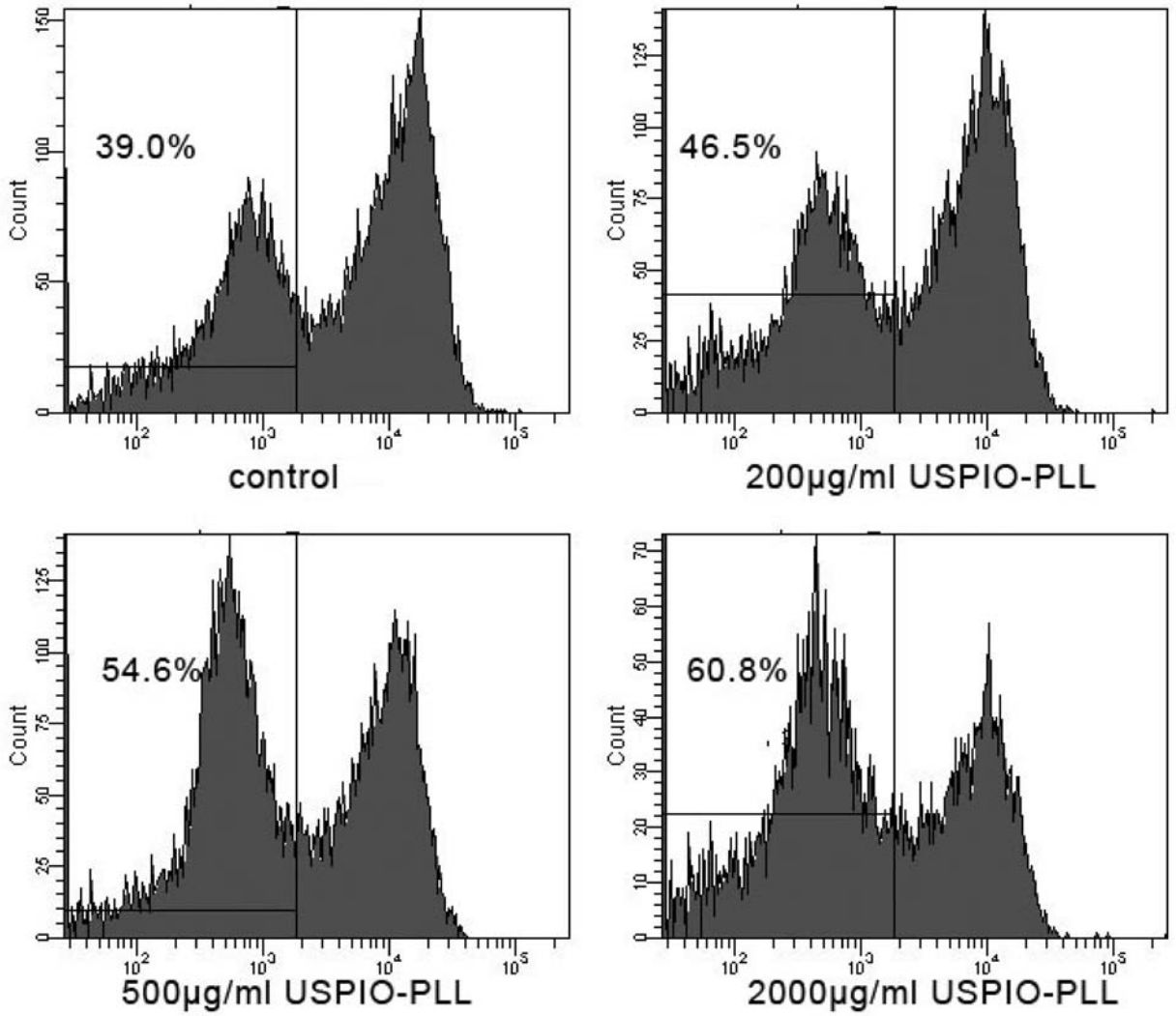

Figure 7 Change of MMP induced by USPIO labeling. After the cells were incubated with different concentrations of USPIO for 24 h, MMP was assessed using cationic dye Rhodamine 123 through flow cytometry. Percentage of cells with low MMP is shown. Each figure is representative of at least three experiments

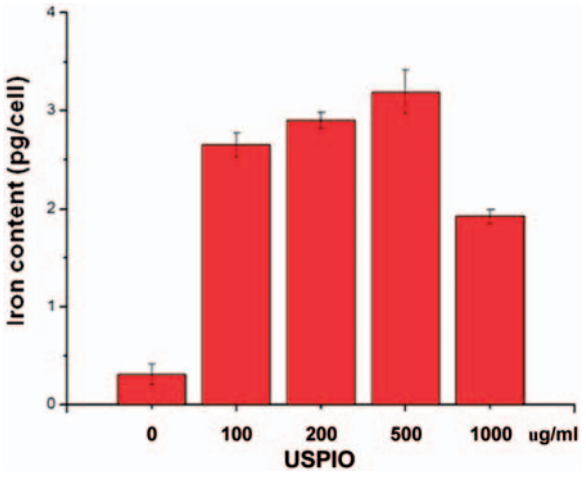

Figure 8 Cellular iron content of USPIO-labeled DCs. DCs were incubated with the indicated concentrations of USPIO for 24 h. For each sample, 1×10^6 cells were collected for AAS assay, and then the mean iron content in each individual cell was further calculated. The graph represents the mean of three experiments. (A color version of this figure is available in the online journal)

concentration until it increased to 2000 μg/mL which induced DCs death by necrosis instead of apoptosis. The change of MMP has been implicated as a key mechanism underlying both necrotic and apoptotic cell death, and the switch from necrotic to apoptotic cell death is dependent on ATP supply.[30] Our data showed that the MMP of the labeled DCs decreased with the increase of USPIO incubation concentration, suggesting a participation of MMP decrease in USPIO induced cell necrosis. The reason why SPIO and USPIO induced two different modes of cell death may be that they exhibit different diameters. Compared with SPIO, USPIO is so small that it can interfere with the ATP production pathway, such as glycolysis, resulting in ATP shortage and cell necrosis. However, different cell types, processing conditions, and labeling methods may also be involved. Moreover, different cell types, processing conditions, and labeling methods may also be involved. However, the fact that 200–1000 μg/mL of USPIO were able to cause MMP decrease but insufficient to trigger necrosis suggests that there might be some other ways involved in DCs necrosis or a threshold of MMP decrease induced necrosis.

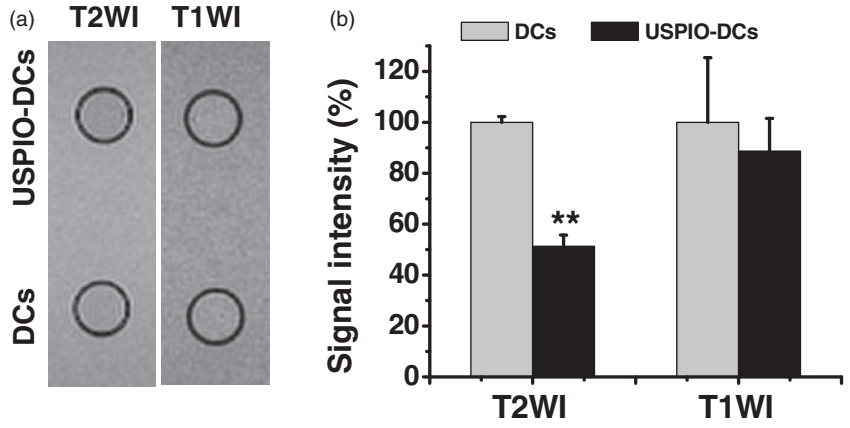

Figure 9 *In vitro* MRI of USPIO-labeled DCs. DCs (1×10^6 cell/ml) were exposed to 200 μg/ml USPIO for 24 h. (a) Same number of unlabeled DCs were set as control. Labeled DCs did not make any difference to signal intensity in T1WI sequence (right panel) but showed lower signal intensity in T2WI sequence (left panel) compared to control. (b) Then the MRI results were quantitativly analyzed

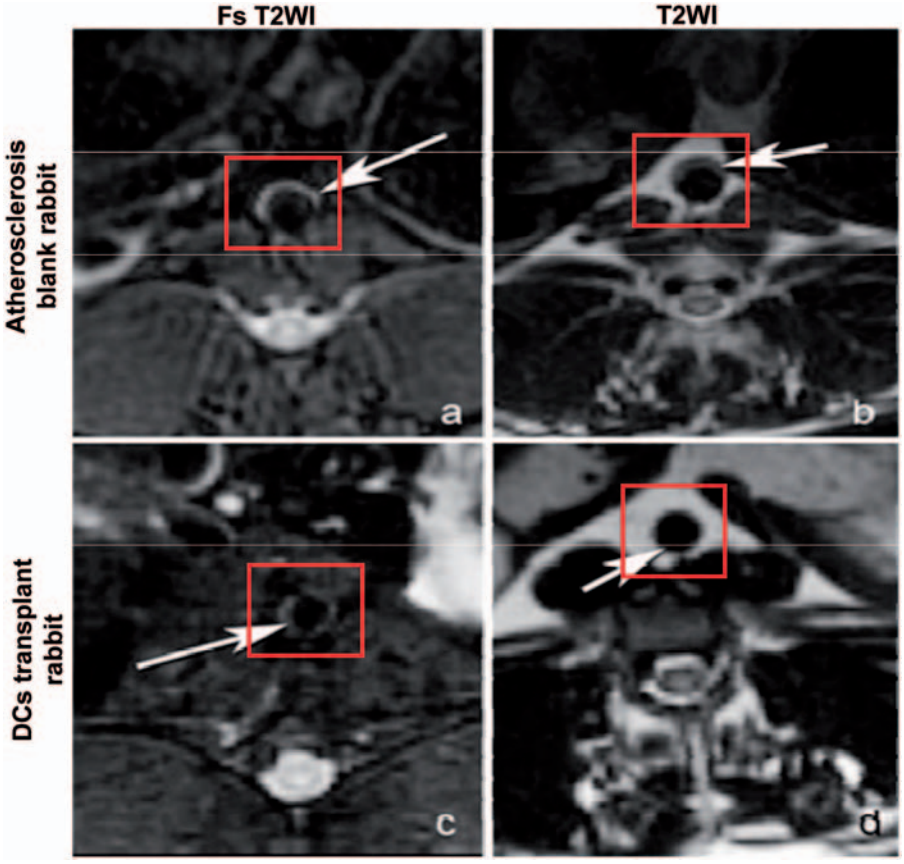

Figure 10 *In vivo* MRI tracking of USPIO-labeled DCs. Two sequences (fs T2WI and T2WI) of MRI were performed. DCs transplanted rabbits got decreased signal intensity (lower luminance) in abdominal aorta (the area within the red rectangle) than atherosclerosis that are blank in both sequence. (A color version of this figure is available in the online journal)

In addition, that control cells have some proportion of apoptosis may relate with our conditions of induction of differentiation which also may be involved in the appearance of the two peak values in the MMP assay. Also the coexistence of mature DCs and immature DCs may contribute to this.

The pathological process of atherosclerosis plaque formation can be divided into four stages: (1) blood vessel endothelium injuries, (2) intima thickening, (3) aging and vulnerable, and (4) rupture and embolization. Hadi's study showed that after fed with high-fat diet for 10 weeks, the blood fat level of rabbits rose significantly accompanied with plaque formation at the aortic arch.[31] We fed the rabbits with high-fat diet for 12 weeks and injected BSA into the model regularly for activating the immune response to

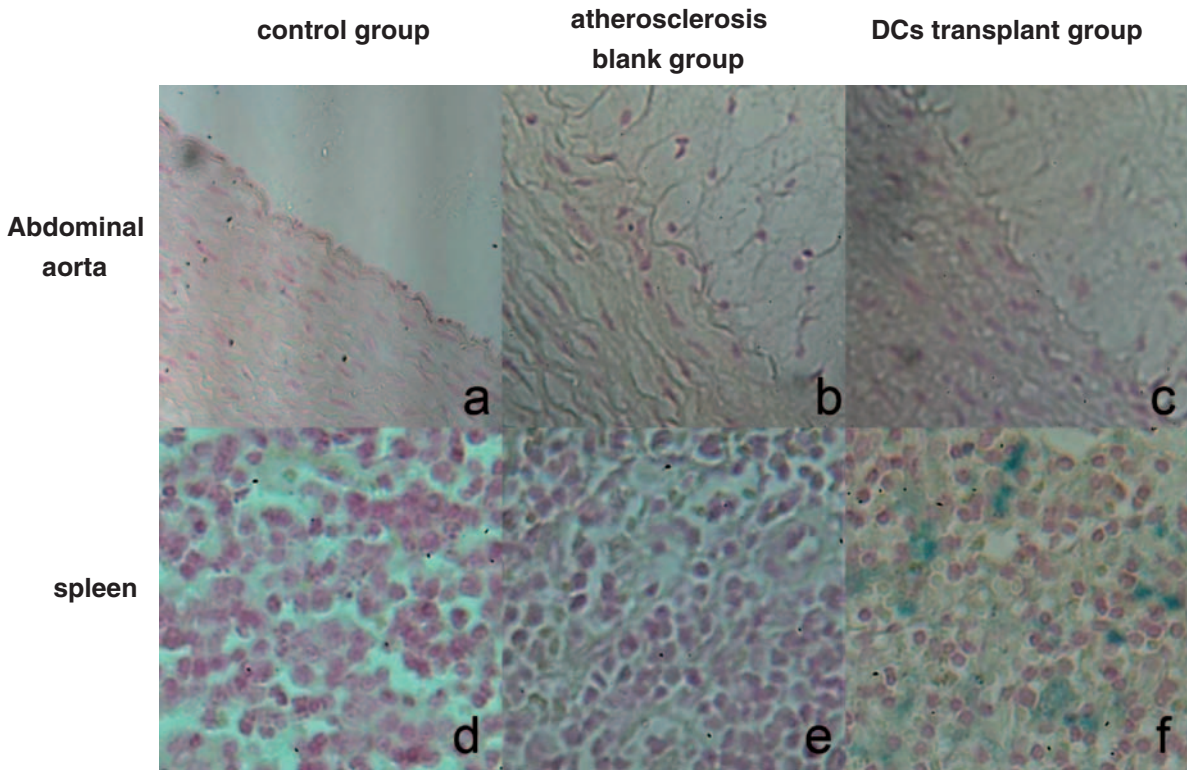

Figure 11 Detection of USPIO-labeled DCs in rabbits *in vivo*. Abdominal aortas (a–c) and spleen (d–f) of control rabbits, atherosclerosis blank, rabbits and DCs transplant rabbits were stained with Prussian blue. Rabbits were transplanted with 200 μg/ml USPIO-labeled DCs for seven days. (A color version of this figure is available in the online journal)

accelerate the plaque formation. Vascular cross-section observation and MRI detection both showed that our rabbit models were at the end of the intima thickening stage.

In general, low concentrations of USPIO (50–500 μg/mL) have no cytotoxicity to rabbit DCs while high concentrations (>500 μg/mL) induced some decrease of DC viability via mitochondria-dependent necrosis instead of apoptosis. A 200 μg/mL USPIO is ideal to effectively label rabbit DCs for MRI tracing *in vivo* without a threat to cell viability. MR imaging (T2WI and fs T2WI sequence) can efficiently track USPIO-labeled DCs existing in rabbit abdominal artery plaques after 24 h of transplant and in spleen after one week detected by Prussian blue staining of tissue sections. Our results revealed a feasible method for tracing transplanted DCs *in vivo*.

Author contributions: All authors participated in the completion of the manuscript. JZ and F-YY conducted most of the experiments and wrote the manuscript, W-LC supplied critical reagents and contributed to the design and review of the study, and QZ and K-RY contributed to the MRI experiments.

ACKNOWLEDGEMENTS

USPIO (Carboxydextran coated Fe_2O_3, $\varphi = 30–50$ nm) was provided by Professor Xu Yikai (Department of Medical Imaging Center, Nan Fang Hospital, Southern Medical University, No. 1838 Guangzhou Avenue North, Guangzhou, Guangdong, 510515, China). This study was supported by the National Basic Research Program of China (2011CB910402; 2010CB732602), the program for Changjiang Scholars and Innovative Research Team in University (IRT0829), National Natural Science Foundation of China (31170250).

REFERENCES

1. Greaves DR, Channon KM. Inflammation and immune responses in atherosclerosis. *Trends Immunol* 2002;**23**:535–41
2. Stoll G, Bendszus M. Inflammation and atherosclerosis: novel insights into plaque formation and destabilization. *Stroke* 2006;**37**:1923–32
3. Woollard KJ, Geissmann F. Monocytes in atherosclerosis: subsets and functions. *Nat Rev Cardiol* 2010;**7**:77–86
4. Van Vré EA, Bosmans JM, Van Brussel I, Maris M, De Meyer GR, Van Schil PE, Vrints CJ, Bult H. Immunohistochemical characterisation of dendritic cells in human atherosclerotic lesions: possible pitfalls. *Pathology* 2011;**43**:239–47
5. Alvarez D, Vollmann EH, von Andrian UH. Mechanisms and consequences of dendritic cell migration. *Immunity* 2008;**29**:325–42
6. Massberg S, Schaerli P, Knezevic-Maramica I, Köllnberger M, Tubo N, Moseman EA, Huff IV, Junt T, Wagers AJ, Mazo IB, von Andrian UH. Immunosurveillance by hematopoietic progenitor cells trafficking through blood, lymph, and peripheral tissues. *Cell* 2007;**131**:994–1008
7. Luo Y, Liang C, Xu C, Jia Q, Huang D, Chen L, Wang K, Wu Z, Ge J. Ciglitazone inhibits oxidized-low density lipoprotein induced immune maturation of dendritic cells. *J Cardiovasc Pharmacol* 2004;**44**:381–5
8. Price CL, Sharp PS, North ME, Rainbow SJ, Knight SC. Advanced glycation end products modulate the maturation and function of peripheral blood dendritic cells. *Diabetes* 2004;**53**:1452–8

9. Van Vré EA, Bult H, Hoymans VY, Van Tendeloo VF, Vrints CJ, Bosmans JM. Human C-reactive protein activates monocyte-derived dendritic cells and induces dendritic cell-mediated T-cell activation. *Arterioscler Thromb Vasc Biol* 2008;**28**:511–8
10. MartIn-Fontecha A, Sebastiani S, Höpken UE, Uguccioni M, Lipp M, Lanzavecchia A, Sallusto F. Regulation of dendritic cell migration to the draining lymph node: impact on T lymphocyte traffic and priming. *J Exp Med* 2003;**198**:615–21
11. Niessner A, Weyand CM. Dendritic cells in atherosclerotic disease. *Clin Immunol* 2010;**134**:25–32
12. Liu P, Yu YR, Spencer JA, Johnson AE, Vallanat CT, Fong AM, Patterson C, Patel DD. CX3CR1 deficiency impairs dendritic cell accumulation in arterial intima and reduces atherosclerotic burden. *Arterioscler Thromb Vasc Biol* 2008;**28**:243–50
13. Bobryshev YV. Dendritic cells in atherosclerosis: current status of the problem and clinical relevance. *Eur Heart J* 2005;**26**:1700–4
14. Modo M, Cash D, Mellodew K, Williams SC, Fraser SE, Meade TJ, Price J, Hodges H. Tracking transplanted stem cell migration using bifunctional, contrast agent-enhanced, magnetic resonance imaging. *Neuroimage* 2002;**17**:803–11
15. Higuchi T, Anton M, Dumler K, Seidl S, Pelisek J, Saraste A, Welling A, Hofmann F, Oostendorp RA, Gansbacher B, Nekolla SG, Bengel FM, Botnar RM, Schwaiger M. Combined reporter gene PET and iron oxide MRI for monitoring survival and localization of transplanted cells in the rat heart. *J Nucl Med* 2009;**50**:1088–94
16. Weissleder R, Elizondo G, Wittenberg J, Rabito CA, Bengele HH, Josephson L. Ultrasmall superparamagnetic iron oxide: characterization of a new class of contrast agents for MR imaging. *Radiology* 1990;**175**:489–93
17. Anzai Y, Prince MR, Chenevert TL, Maki JH, Londy F, London M, McLachlan SJ. MR angiography with an ultrasmall superparamagnetic iron oxide blood pool agent. *J Magn Reson Imaging* 1997;**7**:209–14
18. Bengel FM, Schachinger V, Dimmeler S. Cell-based therapies and imaging in cardiology. *Eur J Nucl Med Mol Imaging* 2005;**32**:S404–16
19. Bulte JW, Kraitchman DL. Iron oxide MR contrast agents for molecular and cellular imaging. *NMR Biomed* 2004;**17**:484–99
20. Na HB, Song IC, Hyeon T. Inorganic Nanoparticles for MRI Contrast Agents. *Adv Mater* 2009;**21**:2133–48
21. Lalande C, Miraux S, Derkaoui SM, Mornet S, Bareille R, Fricain JC, Franconi JM, Le Visage C, Letourneur D, Amédée J, Bouzier-Sore AK. Magnetic resonance imaging tracking of human adipose derived stromal cells within three-dimensional scaffolds for bone tissue engineering. *Eur Cell Mater* 2011;**21**:341–54
22. Yu MX, Chen WL, Zhou Q, Gao P. Study on ASTC-a-1 cells labeled with superparamagnetic iron oxide and its magnetic resonance imaging. *Exp Biol Med* 2010;**235**:1053–61
23. Babic M, Horák D, Trchová M, Jendelová P, Glogarová K, Lesný P, Herynek V, Hájek M, Syková E. Poly(L-lysine)-modified iron oxide nanoparticles for stem cell labeling. *Bioconjug Chem* 2008;**19**:740–50
24. Shapiro EM, Sharer K, Skrtic S, Koretsky AP. *In vivo* detection of single cells by MRI. *Magn Reson Med* 2006;**55**:242–9
25. Himes N, Min JY, Lee R, Brown C, Shea J, Huang X, Xiao YF, Morgan JP, Burstein D, Oettgen P. *In vivo* MRI of embryonic stem cells in a mouse model of myocardial infarction. *Magn Reson Med* 2004;**52**:1214–9
26. Yang C, Canton G, Yuan C, Ferguson M, Hatsukami TS, Tang D. Impact of flow rates in a cardiac cycle on correlations between advanced human carotid plaque progression and mechanical flow shear stress and plaque wall stress. *Biomed Eng Online* 2011;**10**:61–71
27. Esposito L, Saam T, Heider P, Bockelbrink A, Pelisek J, Sepp D, Feurer R, Winkler C, Liebig T, Holzer K, Pauly O, Sadikovic S, Hemmer B, Poppert H. MRI plaque imaging reveals high-risk carotid plaques especially in diabetic patients irrespective of the degree of stenosis. *BMC Med Imaging* 2010;**10**:27–36
28. Lunov O, Syrovets T, Büchele B, Jiang X, Röcker C, Tron K, Nienhaus GU, Walther P, Mailänder V, Landfester K, Simmet T. The effect of carboxydextran-coated superparamagnetic iron oxide nanoparticles on c-Jun N-terminal kinase-mediated apoptosis in human macrophages. *Biomaterials* 2010;**31**:5063–71
29. Lunov O, Syrovets T, Röcker C, Tron K, Nienhaus GU, Rasche V, Mailänder V, Landfester K, Simmet T. Lysosomal degradation of the carboxydextran shell of coated superparamagnetic iron oxide nanoparticles and the fate of professional phagocytes. *Biomaterials* 2010;**31**:9015–22
30. Kim JS, He L, Lemasters JJ. Mitochondrial permeability transition: a common pathway to necrosis and apoptosis. *Biochem Biophys Res Commun* 2003;**304**:463–70
31. Hadi NR, Al-Amran F, Hussein MA, Rezeg FA. Evaluation of the effects of glimepiride (Amaryl) and repaglinide (novoNorm) on atherosclerosis progression in high cholesterol-fed male rabbits. *J Cardiovasc Dis Res* 2012;**3**:5–11

(Received May 3, 2013, Accepted September 6, 2013)